https://doi.org/10.20965/jrm.2012.p0851

Paper:

Walking-Assistance Apparatus as a Next-Generation Vehicle and Movable Neuro-Rehabilitation Training Appliance

Eiichirou Tanaka[*1], Tadaaki Ikehara[*2], Hirokazu Yusa[*3], Yusuke Sato[*3], Tomohiro Sakurai[*4], Shozo Saegusa[*5], Kazuhisa Ito[*1], and Louis Yuge[*6]

[*1]Department of Machinery and Control Systems, Shibaura Institute of Technology
307 Fukasaku, Minuma-ku, Saitama 337-8570, Japan
E-mail: tanakae@sic.shibaura-it.ac.jp
[*2]Tokyo Metropolitan College of Industrial Technology, Tokyo, Japan
[*3]Former Graduate School of Engineering, Shibaura Institute of Technology, Saitama, Japan
[*4]Graduate School of Engineering, Shibaura Institute of Technology, Saitama, Japan
[*5]Hiroshima University, Higashi-Hiroshima, Japan
[*6]Hiroshima University, Hiroshima, Japan
[Received May 27, 2011; accepted March 21, 2012]

We have developed a prototype for a walking-assistance apparatus that serves as a next-generation vehicle or a movable neuro-rehabilitation training appliance for the elderly or motor palsy patients. Our prototype uses a novel spatial parallel link mechanism with a weight-bearing lift. The flat steps of the apparatus move in parallel with the ground; the apparatus supports complete leg alignment, including the soles of the feet, and assists walking behavior at the ankle, knee, and hip joints simultaneously. To estimate the walking phase of each leg of the user, pressure sensors were attached under the thenar eminence and the heel of the sole and the pressure variation at each sensing point was measured. To determine the direction in which the user is walking, a pressure sensor was attached to the flexible crural link. To adapt to the variations in the user's walking velocity, the stride length and walking cycle while walking with the apparatus were compensated for using the concept of the walking ratio (the stride length times the walking cycle is constant). The apparatus can therefore be controlled in response to the user's intent. We developed a control method for the apparatus by using impedance control, taking into account the dynamics of the apparatus and the user's legs, as well as the assist ratio for the user. By adjusting the natural angular frequency of the desired dynamic equation for the user, our apparatus assists walking according to the user's desired response. Motor palsy patients and those with weak muscles can walk with the assistance of the apparatus. Patients who have ambulation difficulty can also use the apparatus with a weight-bearing lift that we developed. Using the apparatus with this lift helps prevent stumbling and enables walking movement to be input to the brain's motor area. The validity of the weight-bearing lift is confirmed from the results of measured % Maximum Voluntary Contraction (%MVC).

Keywords: walking assistance, neuro-rehabilitation, walking ratio, impedance control, weight bearing

1. Introduction

Japan has experienced a rapid growth in its elderly population in recent years. As people age, their muscle strength tends to decrease. Even if they can walk by themselves, they therefore fatigue easily and their walking motion differs from that of a healthy person. As a result, they are more susceptible to stumbling or falling. With such accidents, they experience a lapse in confidence and may also sustain serious injuries; this can decrease their quality of life.

Various walking chairs [1, 2] proposed thus far as substitutes for wheelchairs negotiate stairs, steep hills, narrow streets, and so on. For the elderly to ease the infirmities of old age or for motor palsy patients, however, it is important for them to walk independently. If they use these proposed devices frequently and lose the opportunity for walking, the elderly age greatly and motor palsy patients find it difficult to recover. An assistive cart [3] is effective for such users as training patients to walk on flat ground, but it is necessary for them to be taught and made to grasp the best walking motion as individuals. An assistive cart is also not adequate for use on stairs and steep hills. Some methods for raising subject's leg by only pressing in the upper calcaneus in his/her palsied foot [4], and by giving electro stimulation to subject's muscle [a] are developed. These devices are small and light-weight but, inputting directly to the muscle excessively is fatiguing for users and risks the danger of injury.

We have developed a walking-assistance apparatus for the elderly or motor palsy patients that promotes independence and helps them regain muscle strength. Until now, walking equipment was generally used for walking support. The use of such equipment, however, tires users quickly because equipment is fixed to the joints of

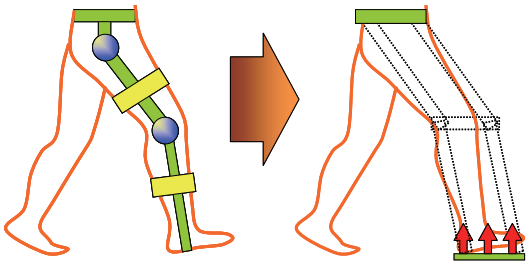

(a) Conventional structure (b) Proposed structure

Fig. 1. Comparison of conventional structure and our proposed structure for walking-assistance apparatus.

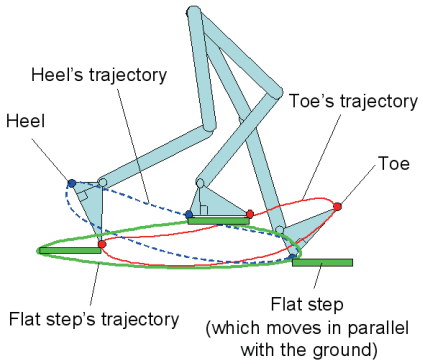

Fig. 2. Trajectory of flat step of apparatus.

the knees and ankles and the patients must turn unnaturally to swing their legs forward when using such equipment. **Fig. 1(a)** illustrates walking-support equipment with a joint drive system of the type that is worn [5–7]. Such walking-support equipments supports the knee and hip joints, which needs an especially large torque during walking but does not support the ankle joint. During long periods of walking, fatigue appears in the Tibialis Anterior (TA) muscle, causing stumbling and dorsiflexion of the ankle [8]. Ikehara therefore developed a device supporting the torques of knee and ankle joints transmitted through flexible shafts [9]. Inoue developed a device [10] that achieves three-joint motion assist by a 1-DOF linkage mechanism alone. Individual users, however, have their own best walking motion, which varies according to the stride length, making it is necessary to adjust the lengths of links in individual cases.

Neuro-rehabilitation, which repairs the neural circuit by directly inputting walking movement to the legs, has recently attracted attention, and numerous training machines have been developed (e.g., [11]). Most of these machines, however, require users to remain stationary during use.

To address the needs and problems above, we developed a walking-assistance apparatus to serve as a next-generation vehicle or a movable neuro-rehabilitation training appliance [12]. Our study is to develop a walking-assistance apparatus that supports the entire leg, including the ankle, knee, and hip joints, while walking, and to assist walking behavior at these joints simultaneously. In our previous study, we confirmed that this apparatus can decrease the activity of the frontal plane muscles by 40%, and that the TA is hardly fatigued even if the user walks for 1 h [12]. We also developed an apparatus as a training device for neuro-rehabilitation exercise in walking for patients who cannot walk or have gait problems. We performed experiments with the prototype and confirmed its effectiveness using electromyography (EMG) measurements.

2. Walking-Assistance Method

We propose a walking-assistance method in which flat steps structurally follow the sole of the foot. That is, the user places the legs on flat steps and is assisted by the walking movement of the entire leg from the sole of the foot, as shown in **Fig. 1(b)**. Key joints and corresponding procedures used in walking are as follows:

a) Hip joint: swings back and forth parallel to the direction of walking movement.

b) Knee joint: swings in a back-and-forth direction.

c) Ankle joint: swings in a back-and-forth direction.

Specifically, the apparatus we developed supports the back-and-forth swinging above, which influences the direction of movement. As shown in **Fig. 2**, flat steps are designed to remain parallel to the ground so that the three joints can be supported simultaneously. In the stance phase of walking, the flat step rests on the ground, while in the swing phase, the flat step is driven according to the lowest position of the sole of each foot. Because posture is controlled when the user stands, this helps prevent stumbling by equipping the apparatus.

3. Designing Walking-Assistance Apparatus

3.1. Application of Spatial Parallel Link Mechanism

We propose a spatial parallel link mechanism to enable the walking-assistance method to be applied. This mechanism connects two parallelograms lengthwise on the front and the side of the user. As shown in **Fig. 3**, the flat step maintains translational motion in the three degrees of freedom (DOF) of the user. As shown in **Fig. 4**, this mechanism is applied to the walking-assistance apparatus; the structure links the parallelograms corresponding to the femoral and crural parts of the leg. To appropriately consider twisting of the ankle, we use a flexible link and spherical joints, as indicated in **Fig. 4**. This link is constructed from a stainless steel plate and rubber to bend and twist with moderate elasticity without buckling because the bending strength of the flexible link has strength equivalent to the aluminum square pipe utilized for other crural links [12]. This makes it durable enough to be pliable in the direction of the link length and strong enough to maintain proper posture.

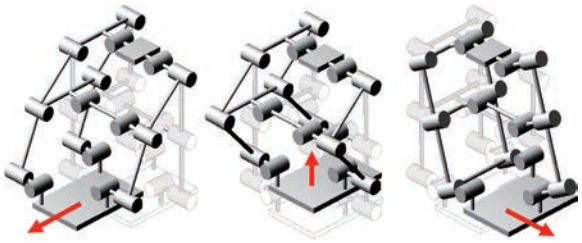

Fig. 3. Three DOFs supported by spatial parallel link mechanism shown for right leg.

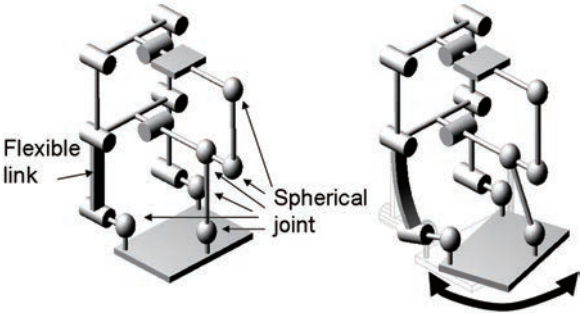

Fig. 4. Flexible link and spherical joints in mechanism enabling twisting, shown for right leg.

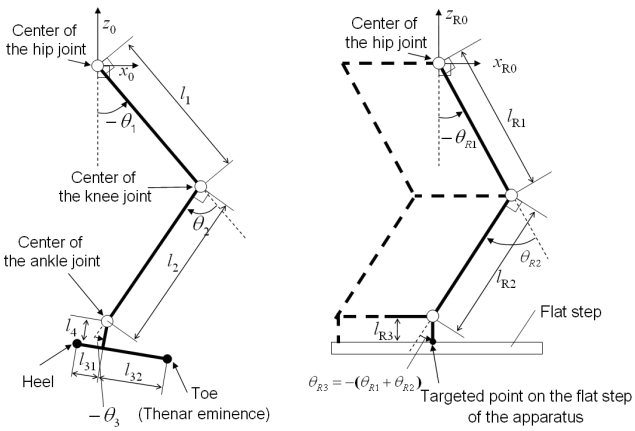

(a) User (b) Apparatus

Fig. 5. Leg models for user and apparatus.

3.2. Selection of Actuator

As mentioned above, the bending strength of the flexible link is almost the same as the aluminum square pipe utilized for other crural links, so calculation error can be ignored by modeling the flexible link as rigid. The calculation model of the apparatus is therefore studied as a two-dimensional model without taking into account the influence of the flexible link in this paper.

Angle variations at each joint (while an able-bodied person is walking) are described in various studies (e.g., [13, 14]). In this paper, we use the values defined in [14] and the walking cycle for an able-bodied person as 1.08 s/step. By using angle variation data for each joint, i.e., hip, knee, and ankle, we calculated a user's trajectory with the leg model shown in **Fig. 5(a)** by using direct kinematics. In contrast, the leg model for the apparatus is defined as shown in **Fig. 5(b)**. The trajectory for the flat step of the apparatus is defined as follows:

1) The trajectories of the heel and the toe (i.e., the thenar eminence) for the user are determined as shown by the thick line in **Fig. 2**.

2) The trajectory for which the z-coordinate in **Fig. 5(a)** is lower, i.e., more downward, than the other is selected in each walking phase.

3) In **Fig. 5(a)**, the x-coordinate of the selected trajectory, i.e., for the thenar eminence or the heel, is shifted as shown in **Fig. 6**. When the z-coordinate of the heel trajectory is lower than that of the toe trajectory in the same walking phase, for example, the targeted point on the flat step in this walking phase is defined by shifting the length of l_{31} from the point on the heel trajectory, as illustrated in **Fig. 6(a)**. In contrast, when the z-coordinate of the toe trajectory is lower than that of the heel trajectory in the same walking phase, the targeted point on the flat step is defined by shifting the length of l_{32} from the point on the toe trajectory, as illustrated in **Fig. 6(b)**.

4) The center of the hip joint of the apparatus is defined as the same point that forms the center of the hip joint of the user. The shifted trajectory is input at the targeted point on the step of the apparatus, as shown in **Fig. 5(b)** and the apparatus is thus controlled according to the trajectory.

To select the actuator, the necessary angular velocity of each joint of the apparatus was calculated by tracking the walking movement of an able-bodied person [14]. The walking cycle was divided into 20 phases and coordinates of the trajectory for the flat step in each walking phase were calculated. Using these results, the values of each angle of the hip and knee joints of the apparatus were calculated using inverse kinematics, i.e., angular velocities of each joint in each walking phase were calculated from the difference of the angle. Referring to **Fig. 5(a)**, the average length of each part of the leg were calculated from reference [b] as follows: Japanese person's average height: 166 cm; thigh length: $l_1 = 395$ mm; shank length: $l_2 = 404$ mm; ankle joint to ground length: $l_4 = 67$ mm; distance from the heel to the line drawn perpendicularly from the center of the ankle joint to the line drawn from the thenar eminence to the heel: $l_{31} = 120$ mm; and distance from the thenar eminence to the line drawn perpendicularly from the center of the ankle joint to the line drawn from the thenar eminence to the heel: $l_{32} = 120$ mm. The apparatus was modeled defining the length of each link set at a maximum $l_{R1} = 400$ mm, $l_{R2} = 490$ mm, and $l_{R3} = 65$ mm.

Figure 7 shows the angular velocity of each human joint and the hip and knee joints of the apparatus in each walking phase. Based on these results, both actuators must output an angular velocity of up to 6 rad/s during

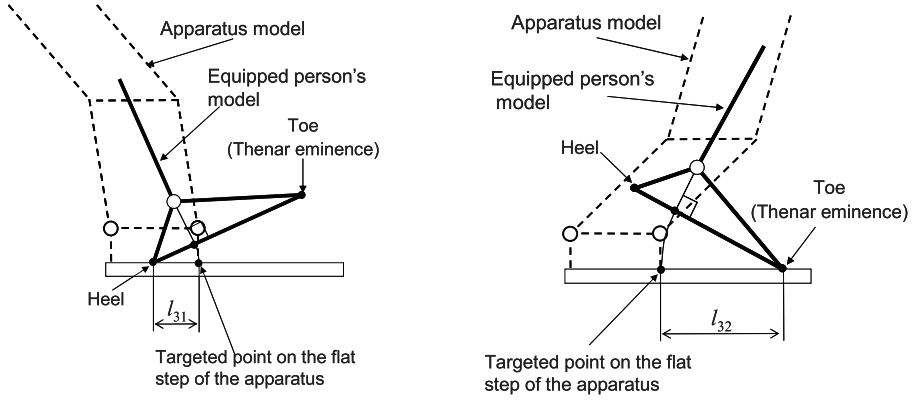

(a) Case 1: when heel trajectory is lower than toe trajectory

(b) Case 2: when toe trajectory is lower than heel trajectory

Fig. 6. Targeted point on flat step of apparatus.

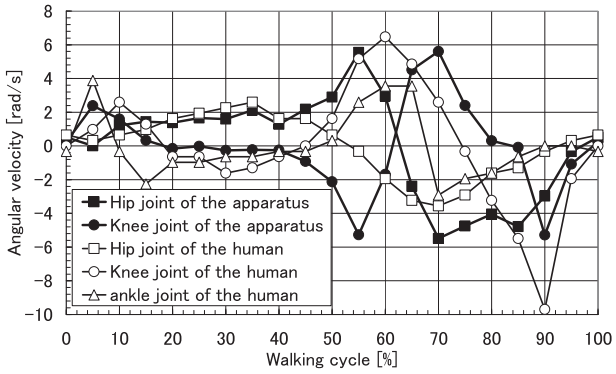

Fig. 7. Comparison of angular velocities of joints between apparatus and human.

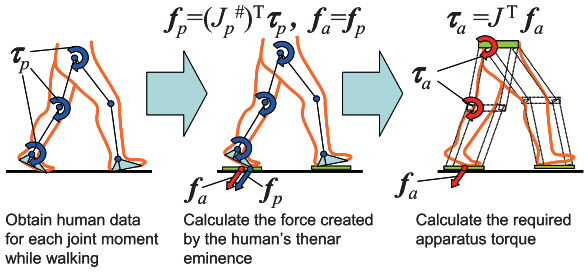

Fig. 8. Calculated necessary torques for apparatus.

walking. The angular velocity of the knee joint is lower in the apparatus than it is in the human, so the utilization of the parallel link mechanism reduces the output angular velocity of the actuator.

We also calculated the necessary output torque of the apparatus from the force that the human outputs at the thenar eminence while walking. Referring to **Fig. 8**, our calculation method is as follows:

1) We obtain the value of joint moment τ_p ($\tau_p = \{\tau_{p\text{-}hip}, \tau_{p\text{-}knee}, \tau_{p\text{-}ankle}\}^T \in \mathrm{R}^3$) from [14], which descried graphs of each human joint, i.e., hip, knee, and ankle, in response to the walking phase.

2) The force that human outputs at the thenar eminence is calculated as force vector $\boldsymbol{f}_p$ as follows:

$$\boldsymbol{f}_p = (J_p^{\#})^T \boldsymbol{\tau}_p, \quad J_p^{\#} = J_p^T \left(J_p J_p^T\right)^{-1}. \quad . \quad (1)$$

where $J_p^{\#}$ is a pseudo-inverse Jacobian matrix and J_p is a Jacobian matrix that relates each human joint angle to its corresponding thenar eminence position. **Fig. 9** shows calculated force vectors and target trajectory. Note that this force is output in the stance phase and is utilized for pushing the foot off the ground.

3) $\boldsymbol{f}_a$ is the necessary output force for the apparatus and is defined using Eq. (1). Each joint torque of apparatus $\boldsymbol{\tau}_a$ is calculated as follows:

$$\boldsymbol{\tau}_a = J^T \boldsymbol{f}_a, \quad \boldsymbol{f}_a = \boldsymbol{f}_p \quad . \quad . \quad . \quad . \quad . \quad . \quad . \quad . \quad (2)$$

where J is a Jacobian matrix for the apparatus.

Calculated results are shown in **Fig. 10**. To achieve the torque required to walk normally, the knee joint actuator must output a force of up to 262 Nm. Based on these results, as summarized in **Table 1**, each actuator's rating power and gear ratio are selected by considering the necessary torque and angular velocity. The efficiency of the gear for the actuator is 75%. The apparatus can drive over 80% of the necessary torque, and the maximum angular velocity required for an able-bodied person to walk can be achieved. **Fig. 11** shows a prototype of the structure.

3.3. Apparatus Control Method

The torque of each actuator was calculated and controlled using a PID controller. The control deviation of the flat step is defined as $\boldsymbol{X}_{in}$ and the electric current input value is defined as $\boldsymbol{I}_{in}$. $\boldsymbol{X}_{in}$ and $\boldsymbol{I}_{in}$ are expressed as follows:

$$\begin{aligned} \boldsymbol{X}_{in} &= \left(K_p + \frac{K_i}{s}\right)(\boldsymbol{X}_d - \boldsymbol{X}) - K_d \dot{\boldsymbol{X}} \\ \boldsymbol{I}_{in} &= K J^T \boldsymbol{X}_{in} + G \end{aligned} \quad . \quad . \quad . \quad . \quad (3)$$

Table 1. Maximum output data of actuator for joints of apparatus.

Joint	Rated power[W]	Gear ratio	Pulley ratio	Total ratio	Max output of angular velocity [rad/s]	Max output torque [N·m]	Ratio with Max output torque and necessary Max torque [%]
Hip	150	126/1	36/36	126/1	6.30	215.46	110
Knee	150	126/1	36/36	126/1	6.30	215.46	82

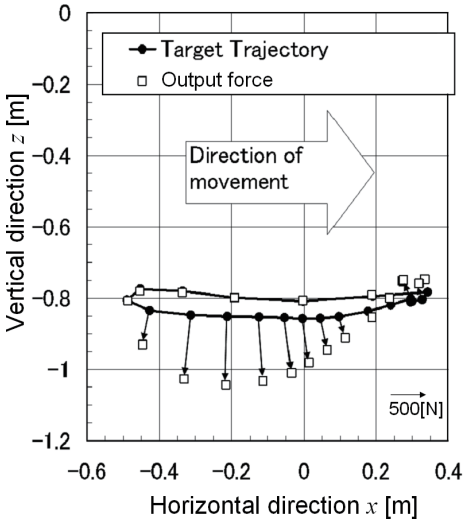

Fig. 9. Target trajectory for flat step and output force vector.

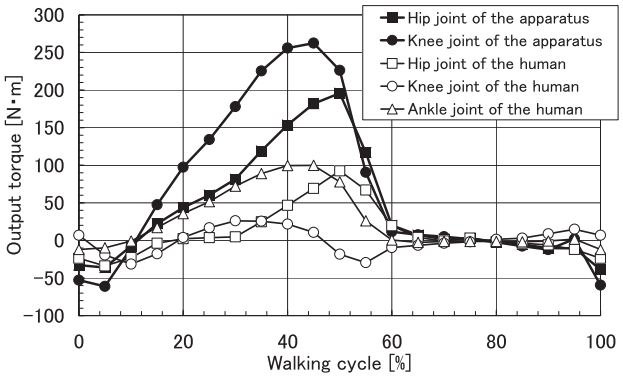

Fig. 10. Joint torque of apparatus exerting human's force.

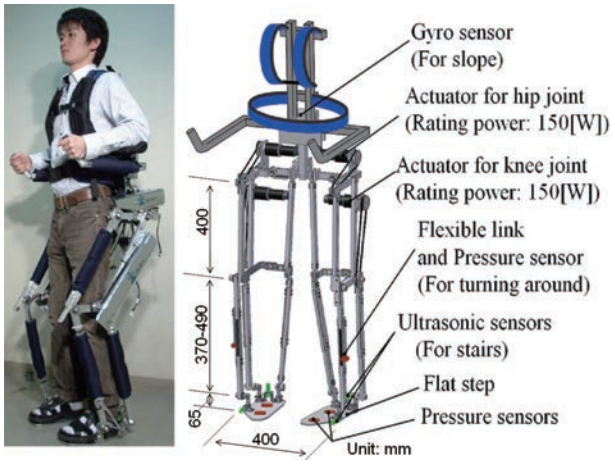

Fig. 11. Structure of mechanism.

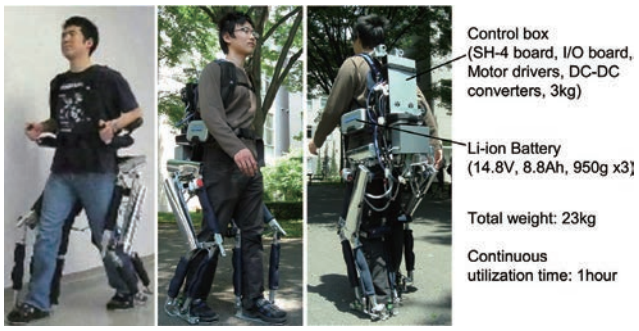

Fig. 12. Example of apparatus utilized as vehicle and self-contained system.

where $\boldsymbol{X}_d$ is the target value; $\boldsymbol{X}$ is the actual measurement value at the center of the flat step; K_p, K_i, and K_d are the gains of PID control; J is the Jacobian matrix from the center of the body to the center of the flat step; K is the diagonal matrix for the proportional coefficient of the torque-electrical current; and G is weight compensation taken into account because of the variation in weight caused by swing and stance phases.

It is also necessary for the control law to consider inertial forces and output forces created by a user. Because the comfort level differs with the user, however, apparatuses must be fine-tuned for individual users. We use the above control law to tune necessary parameters.

Coordinate $\boldsymbol{X}$ of the flat step is calculated by direct kinematics from the encoder value θ, which is attached to each motor; control signal $\boldsymbol{X}_{in}$ is obtained from tracking error $\boldsymbol{X}_d - \boldsymbol{X}$ with control gains K_p, K_i, and K_d. The torque required by each joint is calculated by multiplying $\boldsymbol{X}_{in}$ with the transposed Jacobian matrix J^T. Electrical current input value $\boldsymbol{I}_{in}$ takes into account the weight compensation obtained for each motor driver. Motors are controlled through motor drivers according to the value of $\boldsymbol{I}_{in}$. As a result, the apparatus can assist the user by supplying force according to the deviation of $\boldsymbol{I}_{in}$. Our control system has the SH-4 board as shown in **Fig. 12**. The operating system of the computer is ART-Linux with a control interval of 1 ms. We used three lithium-ion batteries as the power supply for the apparatus as shown in **Fig. 12**.

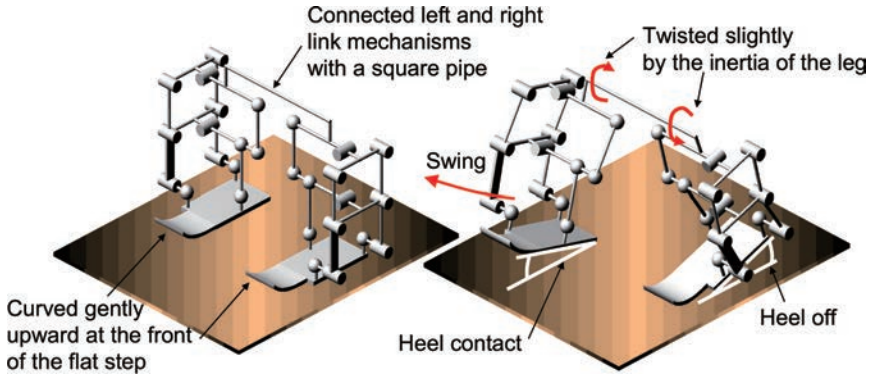

Fig. 13. Link mechanism of walking assistance apparatus.

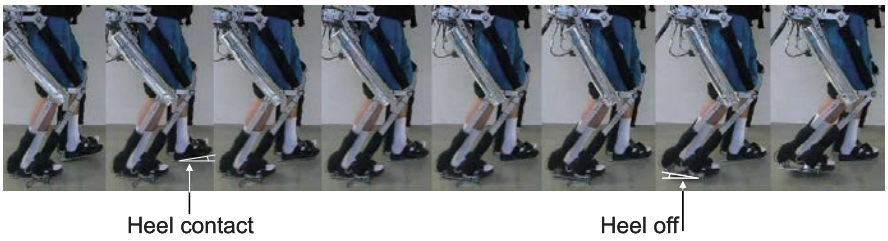

Fig. 14. Walking wearing apparatus during double stance phase (0.07 s/photo).

3.4. Estimating Walking Phase, Slope Angle, and Stair Distance

The user receives assistance power via a sandal attached to the flat step with Velcro tape. The minimum necessary dorsiflexion angle of the ankle joint during walking is ensured by the motion of the flat step, because the target trajectory of the flat step is designed from the minimum height of the trajectories of the heel and thenar eminence during walking. In the later stage of the stance phase, plantar flexion of the ankle joint is promoted by moving the flat step backward as well as the user's instep, which is constrained with the sandal. Visual observations by a third person and videos during walking in the pilot study apparently confirmed heel contact and heel off.

The left and right link mechanisms are connected with a square pipe as shown at left in **Fig. 13**. During walking wearing the apparatus, the connected square pipe is twisted slightly by the inertia of the legs, preventing an inclined flat step. When, for example, the walking phase is at the end of the swing phase, the toe of the flat step is directed upward and the heel of the flat step contacts the ground easily. In contrast, to realize heel off, the front of both flat steps is curved gently upward. **Fig. 14** shows walking wearing the apparatus during the double stance phase. As shown in **Fig. 14**, the left flat step is inclined slightly according to the measured data of the sole pressure sensor as shown in **Fig. 26**, as will hereinafter be described in detail. It was confirmed that the user can achieve heel contact. From the seventh picture from the left in **Fig. 14**, using the curved flat step enables the user to heel off.

To estimate the walking phase of the user's leg, pressure sensors were attached under the thenar eminence and the heel and the pressure variation at each sensing point

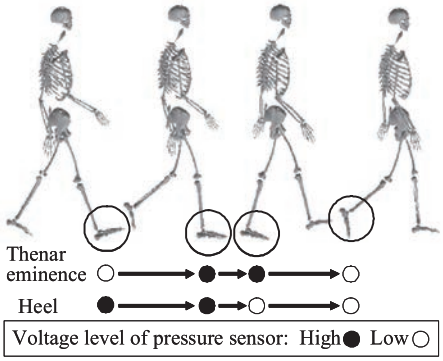

Fig. 15. Measurement of walking phase.

was measured. The sensor was constructed by sandwiching pressure-sensitive conductive rubber 0.5 mm thick within thin copper sheet. Its output voltage was 0–5 V, which is obtained using a partial pressure circuit. Because the sensor is attached to the insole of the shoe, pressure can only be measured with footgears such as a sandal. **Fig. 15** illustrates pressure conditions under the thenar eminence and the heel in the walking phase. The stance phase is estimated by dividing the walking phase into the four distinct steps shown in the figure. By specifying the target value of the step according to each phase, control corresponds to the behavior of the user, which in turn improves safety. In the case of a system malfunction or an emergency, a direct stop switch was also incorporated into the apparatus.

To determine the direction in which the user was walking, pressure sensors were also attached to the flexible crural link. Given the parallel link mechanism, a gyro sensor attached to the back of the apparatus measured the slope angle of the surface on which the user was standing.

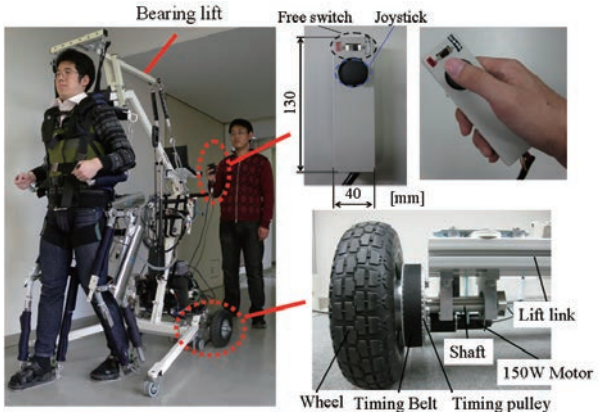

Fig. 16. Photos of the apparatus and weight bearing lift.

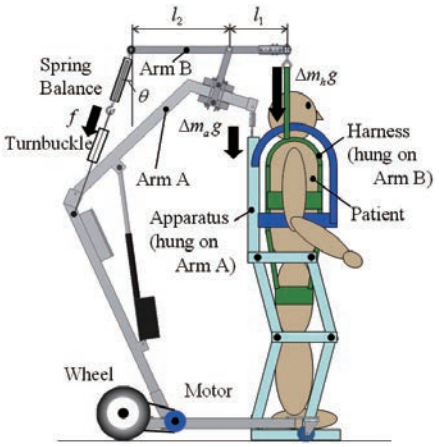

Fig. 17. Mechanism of the weight bearing lift.

To measure the distance between flat steps and stairs, ultrasonic sensors were attached to the toe and heel of the flat step. If the foot in the swing phase is about to hit the edge of a stair, the sensor detects it and hitting the stair is prevented. The user can thus walk on stairs without fear of stumbling or falling.

3.5. Weight-Bearing Lift for Movable Neuro-Rehabilitation Training

Users, including the elderly, who can walk independently can use the apparatus independently. In contrast, it is difficult for those with ambulation difficulty or unable to walk independently to use the apparatus independently because such users are more likely to stumble, making it necessary to support the user's posture. A weight-bearing lift is effective for using apparatus power effectively. As shown in **Figs. 16** and **17**, we developed a weight-bearing lift with two arms, A and B, that can bear the combined weight of the user and the apparatus. As shown in **Fig. 16**, this lift is controlled with a joystick that specifies where the helper or the user wants to go.

Arm A bears the weight of the apparatus (**Fig. 17**) since the apparatus is fixed on arm A. The weight-bearing lift has wheels so that the apparatus and lift can be used while moving. A helper controls the weight-bearing lift from behind at a speed suitable to the patient's needs. Arm A bears 150 kg, which is more than sufficient to support the apparatus's total weight of 20 kg. The arm has actuators that can be adjusted to the height of the apparatus.

Arm B bears the weight of the patient and is attached to arm A. The patient wears a harness hung from a hook at one end of arm B, which was designed to bear a weight of up to 100 kg and can be adjusted to the patient's height, i.e., up to 180 cm.

Weight borne by the user, $\Delta m_{human} g$ [N], is calculated as follows:

$$\Delta m_{human} g = f \frac{l_2 \cos\theta}{l_1} \quad \ldots\ldots\ldots\ldots \quad (4)$$

where f is the tension measured using the spring balance (**Fig. 15**), l_1 is the length from the arm B fulcrum point to the point where the user is positioned, and l_2 is the length from the arm B fulcrum point to the point connected to the spring balance.

The weight-bearing lift enables the patient to feel safer while using the apparatus because the apparatus is fixed on arm A and the patient is supported by arm B, thus preventing the patient from stumbling or falling.

4. Compensation Method for Adapting to Various Walking Velocities

4.1. Walking Ratio

For the elderly and others who can walk without assistance, it is important to promote walking as an exercise to maintain good health. Therefore, we propose utilizing our apparatus as a next-generation vehicle for such exercise and for leisure, as shown in **Fig. 12**, although we note that many of these locations may have varying slopes or stairs. To successfully use our apparatus as a vehicle, it should be able to be adapted to various walking velocities. We therefore propose a new compensation method that uses walking ratio a, represented as follows:

$$a = \frac{lp}{120} \text{ [m/step/min]} \quad \ldots\ldots\ldots\ldots \quad (5)$$

where l [m] is the stride length and p [s/step] is the walking cycle. The value of a is generally 0.006 m/step/min, as detailed in reference [13].

Using this equation, we have developed three control methods that adapt to different walking velocities. Here, we keep p in the range of 1.08 to 2.16 s/step, because 1.08 s/step is the average value recorded for able-bodied persons, as noted above. The maximum value of l is calculated from the target trajectory for each user, which was calculated from the data of each length between the joints of the user and each item of angle variation data [14] by using direct kinematics. The three control methods are as follows:

(a) l is measured during walking using the apparatus, and the target value of p, which is calculated from Eq. (5), is compensated for

$$p = \frac{120a}{l_{measured}}. \quad \ldots\ldots\ldots\ldots \quad (6)$$

(b) p is measured during walking using the apparatus, and the target trajectory is compensated for by multiplying it by the ratio of target value l, which is calculated from Eq. (5) and its maximum value.

$$l = \frac{120a}{p_{measured}}. \quad \ldots\ldots\ldots\ldots \quad (7)$$

(c) If the user wants to walk faster or slower, the time of double stance phase, T [s] is varied according to the requested walking cycle. The time of the double stance phase, T, which is measured for the user, and the adequate value of p are therefore calculated from the linear relationship between the variation of T and p. Target p and l values are compensated for using Eq. (5).

$$p = \alpha T_{measured} + \beta, \quad l = \frac{120a}{p}. \quad \ldots \quad (8)$$

The target value for ideal walking $\boldsymbol{X}_d = \{X_{dx}\ X_{dy}\ X_{dz}\}^T \in \mathrm{R}^3$ was determined along the calculated ideal trajectory as mentioned in Section 3.2 and shown in **Fig. 16**, according to the user's walking phase. In this paper, for simplification of the program and smooth transition between the different walking phases, the original point of the control model for the apparatus was constantly defined as the center of the hip joint of the apparatus; corresponding to the hip joint of the user, regardless of the walking phase. Furthermore, when $\boldsymbol{X}_{d\text{-}comp}$ was the compensated for trajectory taken into account the influence of the walking ratio a for $\boldsymbol{X}_d$, $\boldsymbol{X}_{d\text{-}comp}$ was determined as follows:

$$\boldsymbol{X}_{d\text{-}comp} = \begin{bmatrix} \dfrac{l}{l_d} & 0 & 0 \\ 0 & 1 & 0 \\ 0 & 0 & 1 \end{bmatrix} \boldsymbol{X}_d \in \mathrm{R}^3$$

where l_d is the targeted maximum stride length, which is the distance between both foot at the start of the double stance phase in the calculated trajectory, as shown in **Fig. 18**, and l is control target stride length, which is calculated by Eq. (7) or (8). In this experiment, the control method was utilized with Eq. (3), and then the control target value was $\boldsymbol{X}_{d\text{-}comp}$.

4.2. Experiments

To confirm the validity of each compensation method noted above, l, p, and velocity while walking with the apparatus were measured. Subjects were interviewed regarding the impression of assisted power for each of the compensation methods. Test subjects were two healthy males, 23 and 25 years old, recorded as Subject A and Subject B, with prior experience in walking with the apparatus. Subjects were given instructions to walk 12 steps, i.e., 6 walking cycles. The first 4 steps were accelerated, the middle 4 steps were at maximum speed that subjects felt most suitable, and the final 4 steps were decelerated.

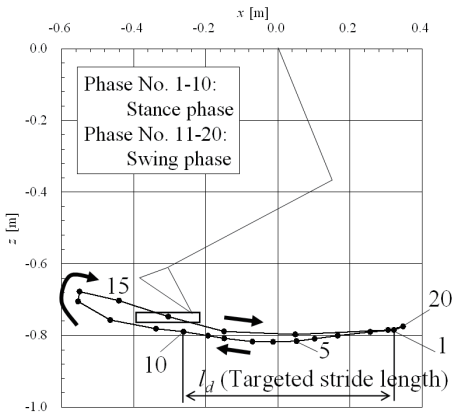

Fig. 18. Sample of ideal target trajectory and targeted stride length.

4.3. Experimental Results

The measured data of l, p, and the walking velocity of the two subjects are shown in **Figs. 19**, **20**, and **21**, respectively. Comparing the results of these figures, similar tendencies are observed in the three graphs. Without compensation, the results vary little. Results of compensation method (a) show that the stride length is longer than that obtained using other results; it also varies little, however. The target of l is constant, so therefore l cannot be diminished by the user.

The walking cycle of compensation method (b) shows almost the same pattern as that of compensation method (c). The target of l is diminished, however, according to p, so walking velocity also decreases. Result ranges of compensation method (c) are the largest of the four studied conditions. Method (c) also shows the best overall opinion on the basis of interview results. We therefore concluded that method (c) is the most effective. When it is adopted in the control program, however, the variation range of T for each subject must be measured and the relationship between T and p grasped previously. In future work, we plan to study the relationships according to age, gender, weight, and other such dimensions.

5. Control Method Considering Dynamics and Assistance Ratio

5.1. Modeling the Apparatus and User

When the user walks with the apparatus controlled using Eq. (3), the flat step can hardly accompany the motion of the user's leg according to the increased walking velocity, because Eq. (3) does not consider the dynamics of the apparatus and the user. To improve the response of the apparatus, we therefore developed a control method that uses impedance control and considers the dynamics of the apparatus and the legs of a user, as well as the assist ratio for the user.

First, each link was labeled as shown in **Fig. 22**, and the apparatus and the user were modeled in two dimensions, as illustrated in **Fig. 23**, by using the following variables:

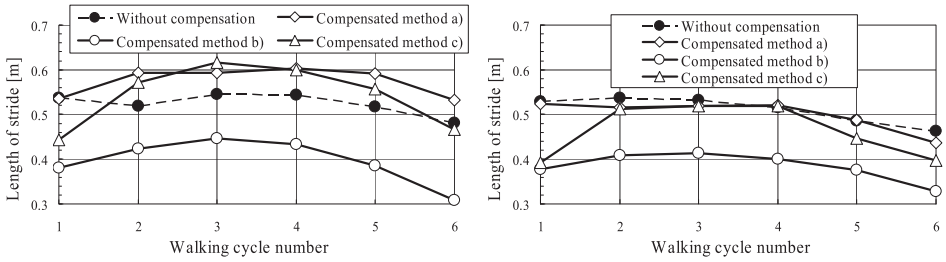

(a) Subject A (b) Subject B

Fig. 19. Comparison of measured variation of stride length under condition of each compensation.

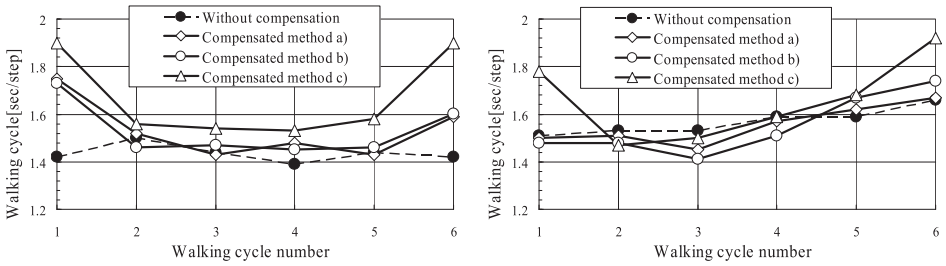

(a) Subject A (b) Subject B

Fig. 20. Comparison of measured variation of walking cycle under condition of each compensation.

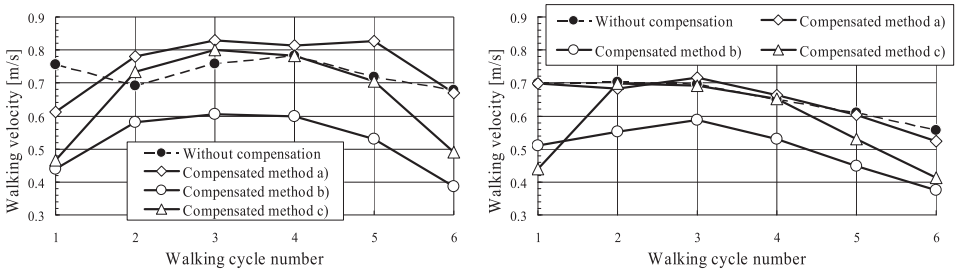

(a) Subject A (b) Subject B

Fig. 21. Comparison of measured variation of walking velocity under condition of each compensation.

Fig. 22. Names of links for modeling.

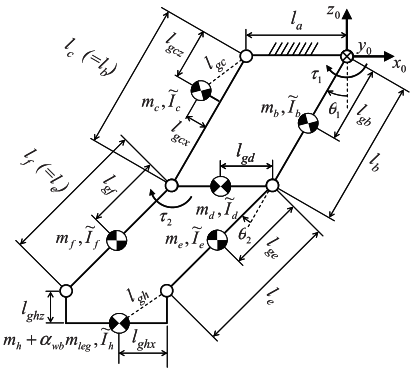

Fig. 23. Apparatus model to make equation (side view).

τ_1 and τ_2 are torques that must be output at the hip and knee joints of the apparatus, respectively.

θ_1 and θ_2 are the angles of the hip and knee joints, respectively, which can be obtained from encoders attached to the end of each motor.

m_b, m_c, m_d, m_e, m_f, and m_h represent the respective masses of each link.

m_{leg} is the mass of the user's leg.

α_{wb} is the weight-bearing ratio for the user, where $\alpha_{wb} = 1 - \frac{\Delta m_{human} g}{m_{human} g}$, $0 \leq \alpha_{wb} \leq 1$.

l_b, l_c, l_d, l_e, l_f, and l_h are the respective lengths of each link.

Table 2. Data of variables for each part of apparatus.

l_b [m]	0.400
l_e [m]	0.490
l_{gb} [m]	0.195
l_{gcx} [m]	0.034
l_{gcz} [m]	0.117
l_{ge} [m]	0.239
l_{gf} [m]	0.194
l_{ghx} [m]	0.061
l_{ghz} [m]	0.041
l_{gh} [m]	0.074

m_b [kg]	0.374
m_c [kg]	1.883
m_d [kg]	0.554
m_e [kg]	0.451
m_f [kg]	0.789
m_h [kg]	1.153

$\tilde{I}_b$ [kgm^2]	0.113
$\tilde{I}_c$ [kgm^2]	0.136
$\tilde{I}_e$ [kgm^2]	0.067
$\tilde{I}_f$ [kgm^2]	0.212

$l_{gb}, l_{gc}, l_{gd}, l_{ge}, l_{gf}$, and $l_{gb}, l_{gc}, l_{gd}, l_{ge}, l_{gf}, l_{gh}$ are the respective lengths to the gravity of each link.

$\tilde{I}_b, \tilde{I}_c, \tilde{I}_d, \tilde{I}_e, \tilde{I}_f$, and $\tilde{I}_h$ are the moments of inertia of each link.

Data of variables for each part of the apparatus are shown in **Table 2**.

Given the above, the torques of each joint of one leg of the apparatus while walking are calculated as follows:

$$\boldsymbol{\tau} = M(\boldsymbol{\theta})\ddot{\boldsymbol{\theta}} + h\left(\dot{\boldsymbol{\theta}}, \boldsymbol{\theta}\right) + g_{ap}(\boldsymbol{\theta}) + \alpha_{gh} g_{human}(\boldsymbol{\theta}) - J^T(\boldsymbol{f}_h + \boldsymbol{f}_r) \in \mathrm{R}^2 \quad \ldots\ldots\ldots (9)$$

where

$$\boldsymbol{\tau} = \{\tau_1, \tau_2\}^T \in \mathrm{R}^2, \quad \boldsymbol{\theta} = \{\theta_1, \theta_2\}^T \in \mathrm{R}^2,$$

$$M(\boldsymbol{\theta}) = \begin{bmatrix} I_1 + I_2 + 2RC_2 & I_2 + 2RC_2 \\ I_2 + 2RC_2 & I_2 \end{bmatrix} \in \mathrm{R}^{2\times 2},$$

$$h\left(\dot{\boldsymbol{\theta}}, \boldsymbol{\theta}\right) = \begin{Bmatrix} -2RS_2\dot{\theta}_1\dot{\theta}_2 - RS_2\dot{\theta}_2^2 \\ RS_2\dot{\theta}_1^2 \end{Bmatrix} \in \mathrm{R}^2,$$

$$I_1 = m_b l_{gb}^2 + m_c l_{gc}^2 + \left(m_d + m_e + m_f + m_h + \alpha_{wb} m_{leg}\right) l_b^2 + \tilde{I}_b + \tilde{I}_c,$$

$$I_2 = m_e l_{ge}^2 + m_f l_{gf}^2 + m_h l_e^2 + \alpha_{wb} m_{leg} l_e^2 + \tilde{I}_e + \tilde{I}_f,$$

$$R = \left(m_e l_{ge} + m_f l_{gf} + m_h l_e + \alpha_{wb} m_{leg} l_e\right) l_b.$$

$g_{ap}(\theta)$ is the gravity compensation for one leg of the apparatus,

$$g_{ap}(\boldsymbol{\theta}) = \begin{Bmatrix} [\{m_b l_{gb} + m_c l_{gcz} + \left(m_d + m_e + m_f + m_h\right) l_b\} S_1 \\ \quad + \left(m_e l_{ge} + m_f l_{gf} + m_h l_e\right) S_{12}]g \\ \left(m_e l_{ge} + m_f l_{gf} + m_h l_e\right) S_{12} g \end{Bmatrix} \in \mathrm{R}^2. \quad \ldots\ldots\ldots (10)$$

α_{gh} is the gravity compensation ratio for one leg, where $0 \leq \alpha_{gh} \leq 1$.

$g_{human}(\theta)$ is the gravity compensation for one leg,

$$g_{human}(\boldsymbol{\theta}) = \begin{Bmatrix} \alpha_{gh}\alpha_{wb}\left(m_{leg} l_b S_1 + m_{leg} l_e S_{12}\right) g \\ \alpha_{gh}\alpha_{wb} m_{leg} l_e S_{12} g \end{Bmatrix} \in \mathrm{R}^2,$$

$$J = \begin{bmatrix} \boldsymbol{J_1} & \boldsymbol{J_2} \end{bmatrix} \in \mathrm{R}^{6\times 2}.$$

$\boldsymbol{J_1} \in \mathrm{R}^6$ is the Jacobian matrix from the hip joint of the apparatus to the flat step.

$\boldsymbol{J_2} \in \mathrm{R}^6$ is the Jacobian matrix from the knee joint of the apparatus to the flat step.

$\boldsymbol{f}_h$ is the force that the user must output in order to walk, and $\boldsymbol{f}_h = \left\{f_x \;\; f_y \;\; f_z \;\; 0 \;\; 0 \;\; 0\right\}^T \in \mathrm{R}^6$.

$\boldsymbol{f}_r$ is the floor reaction force in the stance phase, $\boldsymbol{f}_r = \left\{f_{rx} \;\; f_{ry} \;\; f_{rz} \;\; 0 \;\; 0 \;\; 0\right\}^T \in \mathrm{R}^6$.

By using Eq. (9), the dynamics of both the apparatus and the user while walking can be taken into account. The value of α_{gh} is also an assistance ratio, determined according to the condition of the user's leg. $\boldsymbol{f}_r$ is defined as the vector at the center of gravity of link h. As mentioned in Section 4.2, in this paper, the original point of the control model for the apparatus was constantly defined as the center of the hip joint of the apparatus; corresponding to the hip joint of the user, regardless of the walking phase. $\boldsymbol{f}_r$ is used to input calculated data using the three graphs (f_{rx}, f_{ry}, f_{rz}, ordinate: ratio of human weight, abscissa: walking phase) in [13] and the value of the sum of the weight of the apparatus and the user. These values for each parameter change according to the walking phase, especially during the double stance phase.

5.2. Impedance Control Method

By adjusting the value of the natural angular frequency of the desired dynamic equation for the user, as given by Eq. (10), our apparatus can assist walking according to the user's desired response.

$$M_d\ddot{\boldsymbol{p}} + D_d\dot{\boldsymbol{p}}_e + K_d\boldsymbol{p}_e = \boldsymbol{f}_h \in \mathrm{R}^3 \quad \ldots\ldots (11)$$

where $\boldsymbol{p}_e = \boldsymbol{p} - \boldsymbol{p}_d \in \mathrm{R}^3$ is the deviation from the target.

$\boldsymbol{p} = \left\{p_x \;\; p_y \;\; p_z\right\}^T \in \mathrm{R}^3$ is the current position of the flat step.

$\boldsymbol{p}_d = \left\{p_{dx} \;\; p_{dy} \;\; p_{dz}\right\}^T \in \mathrm{R}^3$ is the position of the target varying according to the walking phase of the trajectory.

M_d is the desired mass matrix when the user moves, $M_d = \mathrm{diag}[m_x \;\; m_y \;\; m_z] = \mathrm{diag}[m_d \;\; m_d \;\; m_d] \in \mathrm{R}^{3\times 3}$.

K_d is the desired stiffness matrix when the user moves, $K_d = \mathrm{diag}[k_x \;\; k_y \;\; k_z] = \mathrm{diag}[k_d \;\; k_d \;\; k_d] \in \mathrm{R}^{3\times 3}$.

D_d is the desired damping matrix when the user moves, $D_d = \mathrm{diag}[d_x \;\; d_y \;\; d_z] = \mathrm{diag}[d_d \;\; d_d \;\; d_d] \in \mathrm{R}^{3\times 3}$.

The mass of the user's leg, m_{leg} was calculated by using the mass ratio of weight m_{human} [13], e.g., in the case of Subject A, m_{human} was 70 kg, and $m_{leg} = 0.0725 \times m_{human} = 5.075$ kg, therefore, $m_d = (1 - \alpha_{gh}) m_{leg} = (1 - 0.2) \times 5.075 = 4.06$ kg.

When Eq. (10) and $\ddot{\boldsymbol{p}} = J\ddot{\boldsymbol{\theta}} + \dot{J}\dot{\boldsymbol{\theta}} \in \mathrm{R}^3$ are input to Eq. (9), the output torque of each joint of the apparatus is expressed as follows, without using $\ddot{\boldsymbol{p}}$ and $\boldsymbol{f}_h$ (note that the value of $\ddot{\boldsymbol{\theta}}$ can be obtained from discrete and filtered $\boldsymbol{\theta}$):

$$\boldsymbol{\tau} = M(\boldsymbol{\theta})\ddot{\boldsymbol{\theta}} + h\left(\dot{\boldsymbol{\theta}}, \boldsymbol{\theta}\right) + g_{ap}(\boldsymbol{\theta}) + \alpha_{gh} g_{human}(\boldsymbol{\theta}) - J^T\left[\left\{M_d\left(J\ddot{\boldsymbol{\theta}} + \dot{J}\dot{\boldsymbol{\theta}}\right) + D_d\dot{\boldsymbol{p}}_e + K_d\boldsymbol{p}_e\right\} + \boldsymbol{f}_r\right] \in \mathrm{R}^2 \quad \ldots\ldots (12)$$

Table 3. Subject data.

Subject	Height [cm]	Weight [kg]	Age	Sex
A	172	70	25	Male
B	169	58	24	Male

Table 4. Experiment data of each impedance property.

Exp. No.	Subject	m_d [kg]	k_d [N/m]	d_d [N sec/m]	ω_c [rad/sec]	ζ
A-1	A	4.06	102	40.6	5	1
A-2			199	56.8	7	
A-3			406	81.2	10	
A-4			686	105.6	13	
A-5			9145	121.8	15	
A-6			1173	138.0	17	
A-7			1624	162.4	20	
B-1	B	3.36	84	33.6	5	
B-2			165	47.1	7	
B-3			336	67.3	10	
B-4			569	87.5	13	
B-5			757	100.9	15	
B-6			972	114.4	17	
B-7			1346	134.6	20	

5.3. Hearing and Trajectory Measuring Experiments

To confirm the validity of our new control method, we performed hearing and trajectory measuring experiments during assisted walking, which is controlled using Eq. (11). To adjust the response of the assistance force, the values of natural angular frequency ω_c and damping ratio ζ of the desired dynamic equation for the user are defined as follows:

$$\omega_c = \sqrt{\frac{k_d}{m_d}}, \quad \zeta = \frac{d_d}{2\sqrt{m_d k_d}}.$$

Subjects in our experiments were two able-bodied men with the characteristics summarized in **Table 3**. The value of each m_d was calculated from the weight of each person's leg and assistance ratio $\alpha_{gh} = 20\%$. According to the value of ω_c in the range of 5–20 Hz, k_d and d_d were set to a variety of values, as shown in **Table 4**. Subjects walked in a straight line at a constant velocity with the same target walking cycle of 1.30 s/step, which was the value for which both subjects could walk comfortably while wearing the apparatus.

The results of our experiments are summarized as follows:

- Subjects did not report feeling the weight of the apparatus in any experiment, so the gravity compensation and inertia terms for the apparatus were effective.
- In experiments A-1 and B-1, subjects felt negligible assistance force, so they had to walk using their own strength.
- In experiments A-2 through A-6 and B-2 through B-6, according to the increased value of ω_c, the assistance force also increased.
- Subjects reported that experiments A-5 and B-5, in which $\omega_c = 15$ rad/s, were the easiest to walk.
- Subjects reported that experiments A-7 and B-7, in which $\omega_c = 20$ rad/s, proved difficult to walk because the assistance force was too strong.

The variations of hip and knee motor currents and voltages of sole sensors were measured during walking, and then we calculated output torques. From the seven combinations that we created, the user chose impedance control best suited for walking ($\omega_c = 15$ rad/s). Results compared between targeted and measured torques are shown in **Figs. 24** and **25**. Each walking phase was selected from measured results of each of the sole pressure sensors as shown in **Fig. 26**. Targeted and measured results were almost the same shape. It can therefore be confirmed that this apparatus can adequately assist the user's walking. Due to the output torque limitation of our current motors we are unable to achieve our desired torque of 26 N·m. To remedy this limitation we are considering using a spring mechanism to achieve our desired torque. Increasing the size of the motor is counter productive due to the weight increase of a larger motor and battery.

Figure 27 shows mean results for three walking cycles of each measured trajectory of the flat step. Both trajectories, at $\omega_c = 20$ rad/s, deviated from other trajectories, and we observed that the walking form collapsed. From the figure, the future of the trajectory varied for each subject, but the most effective value of ω_c remained constant. We therefore conclude that the intensity of the assistance force during walking can be adjusted by ω_c. In all experiments, the assistance ratio was $\alpha_{gh} = 20\%$, but it was difficult to confirm whether the value of the assistance ratio is adequate for the user or not because we did not measure muscle activity and the adequate value of the assistance ratio is different according to the age, condition, familiarity with device use or not, usage, and so on. Even though the assistance ratio of the Lokomat (driven gate orthosis) [11] was set to 100 %, muscle activity of the subject was generated [15]. As future work, we aim to clarify the relationship between the assistance force, assistance ratio, and ω_c.

6. Evaluating Effectiveness of Weight-Bearing Lift

To evaluate the effectiveness of the developed weight-bearing lift, the trajectories of the flat step and EMG data of one leg of the user during walking with the apparatus and using the weight-bearing lift were measured. The test subject was a healthy 23-year-old man who was 172 cm tall, weighed 66 kg, and had prior experience in walking using the apparatus. He walked with a walking cycle of 1.30 s/step, which was comfortable for him using the apparatus and weight-bearing lift. The scenarios of the experiment are as follows:

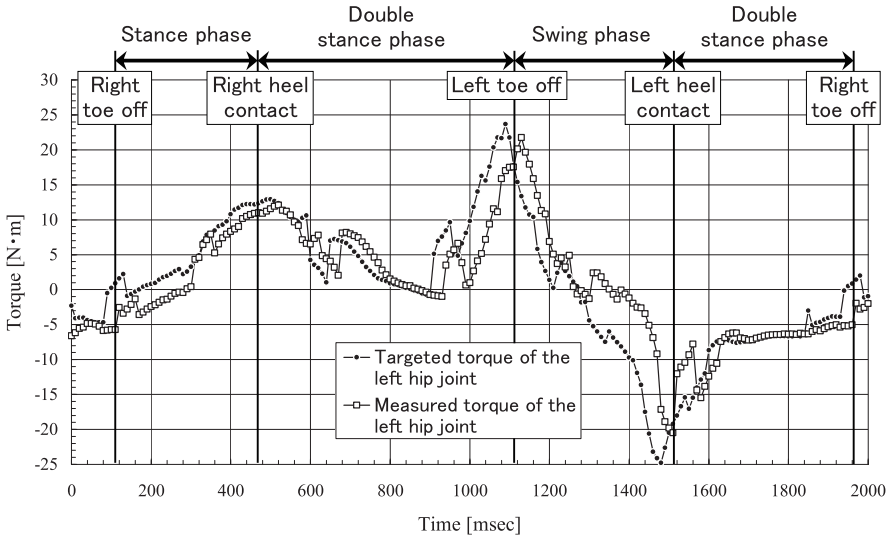

Fig. 24. Comparison between targeted and measured torques of left hip joint during walking.

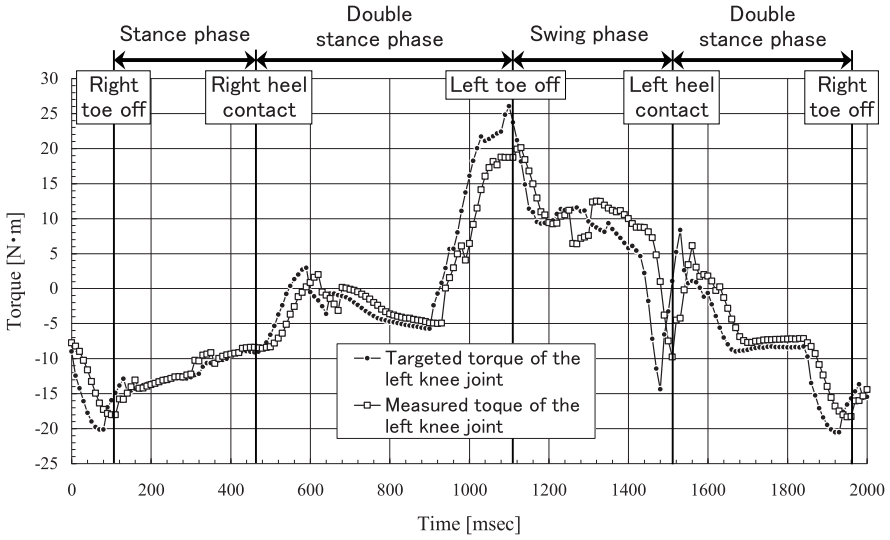

Fig. 25. Comparison between targeted and measured torques of left knee joint during walking.

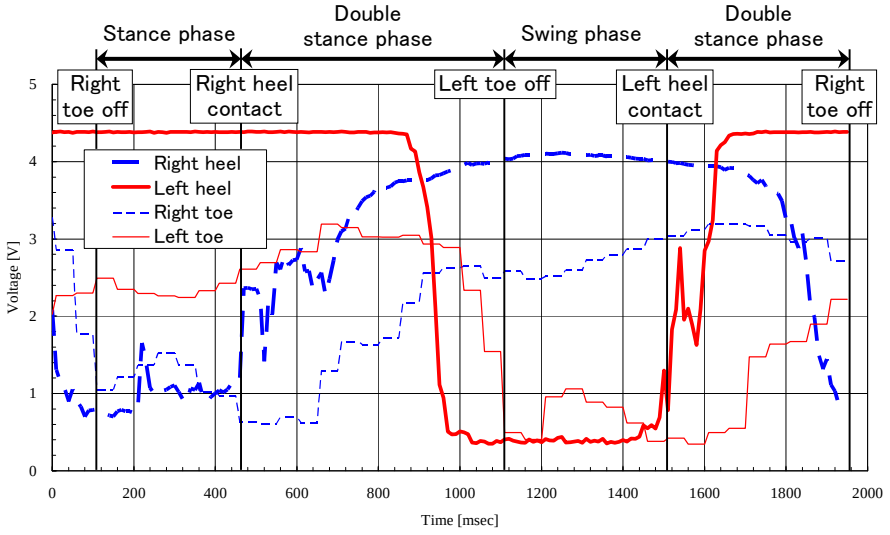

Fig. 26. Measured results of each of measured sole pressure sensors during walking.

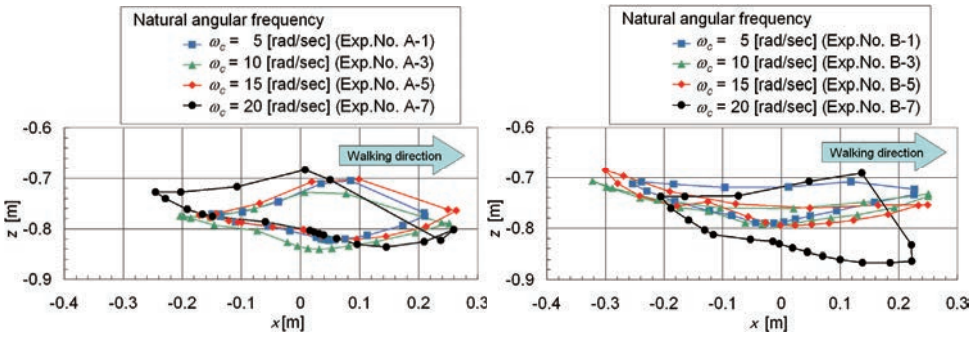

(a) Subject A (b) Subject B

Fig. 27. Measured trajectory of flat step during walking.

(a) Walking with the apparatus without the weight-bearing lift.

(b) Walking with the apparatus and using arm A of the weight-bearing lift, bearing 60% of the apparatus's weight (22 kg).

(c) Walking with the apparatus and using both arms A and B of the weight-bearing lift, bearing 60% of the apparatus's weight (22 kg) and 30% of the subject's weight (66 kg).

In this experiment, the control method also utilized Eq. (3), and the control target value was $\boldsymbol{X}_d$, i.e., it did not taken into account the influence of the walking ratio. The subject walked straight ahead with constant velocity, taking 10 steps and the trajectory and EMG were measured. Mean results of measured trajectories are shown in **Fig. 28**. In the figure, to compare the height of each trajectory in the swing phase, the lowest position was defined as the baseline. Evidently, the height of the trajectory in the swing phase increased according to the weight-bearing condition, but in the final stance phase of conditions (b) and (c), both trajectories were diminished. There is a possibility that even though the user did not push off the ground with much strength, his leg may have shifted from the stance phase to the swing phase.

Measured EMG data was collected from the following four points on the right leg: tibialis anterior muscle (TA), medial head of the gastrocnemius muscle (GMH), rectus femoris muscle (RF), and long head of the biceps femoris muscle (BFL). The distance between electrodes of the EMG sensor was 34 mm, the signal amplified by 1000 times was converted from analog to digital with a sampling time of 1 kHz, sent wirelessly, and recorded with a PC. Integrated EMG (IEMG) at intervals of 0.1 s was calculated from EMG data, and maximum values of IEMG for each step were averaged. Each average was compared with the Maximum Voluntary Contraction (MVC), and thus, the percentage of MVC (%MVC) for each condition was derived.

Figure 29 summarizes results. For our subject, the crural muscles (TA and GMH) are used more actively than the femur muscles (RF and BFL), and the muscle activity can be decreased using the weight-bearing lift. The activity of BFL was especially decreased by using both arms of the weight-bearing lift. By using arm B, the floor reaction force arising from the user's weight decreased, because the user did not have to push off the ground as strongly. The activity of BFL also decreased. The weight-bearing lift can therefore be utilized to adjust the user's load for training. The behavior of pushing off the ground is, however, important in rehabilitation. Hence, in the future, we plan to increase the number of subjects and confirm the relationship between weight-bearing force and activity of the BFL; our goal is to show that our apparatus will be effective in clinical use with motor palsy patients.

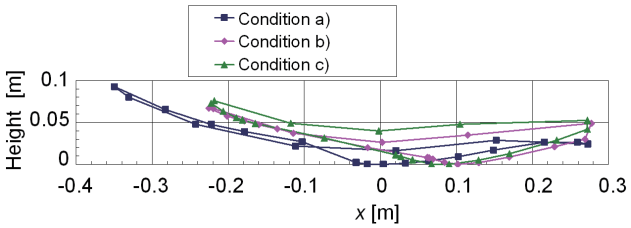

Fig. 28. Measured trajectory of flat step during walking.

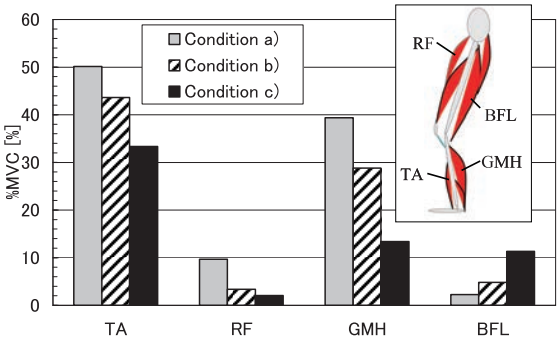

Fig. 29. Comparison of %MVC data of each condition.

7. Conclusions

We have developed a new walking-assistance apparatus for use as a next-generation vehicle or as a movable neuro-rehabilitation device for the elderly or motor palsy

patients. To adapt to variations in walking velocity, we have adopted the concept of the walking ratio to control the apparatus. The dynamics of the apparatus and the abilities of the user have been taken into account in the control mechanism, and we have suggested a method to adjust the assistance force by the natural angular frequency. For patients who cannot walk independently, the weight-bearing lift can successfully bear both the apparatus and the user. Finally, we have confirmed the feasibility of our weight-bearing lift by measuring %MVC. By using the lift together while adjusting adequate bearing weight, the elderly and disabled patients or those requiring rehabilitation can therefore benefit from our apparatus.

References:

[1] Y. Wu et al., "Development of a Power Assist System of a Walking Chair (Proposition of the Speed-Torque Combination Power Assist System)," J. of Robotics and Mechatronics, Vol.17, No.2, pp. 189-197, 2005.

[2] K. Hashimoto et al., "Biped Landing Pattern Modification Method and Walking Experiments in Outdoor Environment," J. of Robotics and Mechatronics, Vol.20, No.5, pp. 775-784, 2008.

[3] K. Miyawaki et al., "Evaluation and Development of Assistive Cart for Matching to User Walking," J. of Robotics and Mechatronics, Vol.19, No.6, pp. 637-645, 2007.

[4] K. Masushita et al., "A Case Study Approach: Walking Assist Scheme Exploiting Somatic Reflex of a Leg-Paralysis Patient," J. of Robotics and Mechatronics, Vol.19, No.6, pp. 629-636, 2007.

[5] K. Yamamoto et al., "Development of Power Assisting Suit for Assisting Nurse Labor," JSME Int. J., Series C, Vol.45, No.3, JSME, pp. 703-711, 2002.

[6] K. Suzuki et al., "Intention-Based Walking Support for Paraplegia Patient," Proc. of the 2005 IEEE Int. Conf. on Systems, Man and Cybernetics (SMC2005), Hawaii, pp. 2707-2713, 2005.

[7] T. Nakamura et al., "Control of Wearable Walking Support System Based on Human-Model and GRF," Proc. of the 22nd Annual Conf. of the Robotics Society of Japan, 1I35, 2004 (in Japanese).

[8] T. Ikehara et al., "Study on Dynamic Balance and Prolonged Walk for Development of Active Auxiliary Walk-Implement," Proc. of the 1st KSME-JSME Joint Int. Conf. on Manufacturing, Machine Design and Tribology (ICMDT), Seoul, KOREA, 2005.

[9] T. Ikehara et al., "Development of Closed-Fitting-Type Walking Assistance Device for Legs with Self-Contained Control System," J. of Robotics and Mechatronics, Vol.22, No.3, pp. 380-390, 2010.

[10] H. Inoue et al., "Development of Walking Assist Machine Using Linkage Mechanism – Mechanism and its Fundamental Motion –," J. of Robotics and Mechatronics, Vol.22, No.2, pp. 189-196, 2010.

[11] G. Colombo et al., "Treadmill training of paraplegic patients using a robotic orthosis," J. of Rehabilitation Research and Development, Vol.37, No.6, pp. 693-700, November/December, 2000.

[12] H. Yusa et al., "Development of a Walking Assistance Apparatus using a Spatial Parallel Link Mechanism and Evaluation of Muscle Activity," Proc. of the 19th IEEE Int. Symposium in Robot and Human Interactive Communication (IEEE Ro-Man 2010), Viareggio, Italy, CD-ROM, 2010.

[13] R. Nakamura et al., "Fundamental Kinesiology, sixth edition," Ishiyaku pubrishers Inc., 2003 (in Japanese).
ISBN: 978-4-263-21153-3

[14] Y. Ehara and S. Yamamoto, "Introduction to Body-Dynamics-Analysis of Gait and Gait Initiation," Ishiyaku publishers Inc., 2002 (in Japanese). ISBN: 4-263-21532-X

[15] S. Aoki et al., "Effect of Guidance Force of Lokomat on Body Weight Supported Training for Restoration of Locomotion, The Institute of Electronics," Information and Communication Engineers, Technical Report, MBE2008-51, pp. 133-138, 2008.

Supporting Online Materials:

[a] NESS L300.
http://www.bioness.com/L300_for_Foot_Drop.php

[b] AIST anthropometric database1991-92 (in Japanese).
http://riodb.ibase.aist.go.jp/dhbodydb/91-92/

Name:
Eiichirou Tanaka

Affiliation:
Associate Professor, Shibaura Institute of Technology

Address:
307 Fukasaku, Minuma-ku, Saitama 337-8570, Japan

Brief Biographical History:
1997- Joined Mechanical Engineering Research Laboratory, Hitachi, Ltd.
2003- Graduated the Interdisciplinary Graduate School of Science and Engineering, Tokyo Institute of Technology
2005- Research Associate, Hiroshima University
2009- Associate Professor, Shibaura Institute of Technology

Main Works:
• "Walking Assistance Apparatus Using a Spatial Parallel Link Mechanism and a Weight Bearing Lift," Proc. of the IEEE Int. Conf. on Rehabilitation Robotics, June 29 to July 1, Zurich, Switzerland, 2011.

Membership in Academic Societies:
• The Japan Society of Mechanical Engineers (JSME)
• The Robotics Society of Japan (RSJ)
• Japan Society for Design Engineering (JSDE)
• Society of Biomechanisms (SOBIM)

Name:
Tadaaki Ikehara

Affiliation:
Associate Professor, Tokyo Metropolitan College of Industrial Technology

Address:
8-17-1 Minami-Senju, Arakawa-ku, Tokyo 116-0003, Japan

Brief Biographical History:
2000 Graduated the Master's Course of Sport Science, Nippon Sport Science University
2008- Lecturer, Tokyo Metropolitan College of Industrial Technology
2011 Graduated the Doctor's Course of Engineering, Hiroshima Univ.

Main Works:
• "Development of a Closed-Fitting-Type Walking Assistance Device on Leg with a Self-Contained Control System," J. of Robotics and Mechatronics, Vol.22, No.3, pp. 380-390, 2010.

Membership in Academic Societies:
• The Japan Society of Mechanical Engineers (JSME)
• Japan Society for Design Engineering (JSDE)
• Japan Society of Physical Education, Health and Sport Sciences

Name:
Hirokazu Yusa

Affiliation:
Former Student of Graduate School of Engineering, Shibaura Institute of Technology

Address:
307 Fukasaku, Minuma-ku, Saitama 337-8570, Japan

Brief Biographical History:
2011 Graduated Graduate School of Engineering, Shibaura Institute of Technology
2011- Joined Sumitomo Heavy Industries, Ltd.

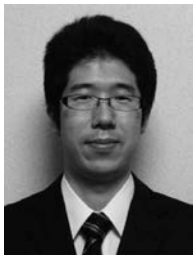

Name:
Yusuke Sato

Affiliation:
Former Student of Graduate School of Engineering, Shibaura Institute of Technology

Address:
307 Fukasaku, Minuma-ku, Saitama 337-8570, Japan

Brief Biographical History:
2011 Graduated Graduate School of Engineering, Shibaura Institute of Technology
2011- Joined CITIZEN FINETECH MIYOTA Co, Ltd.

Name:
Tomohiro Sakurai

Affiliation:
Student of Graduate School of Engineering, Shibaura Institute of Technology

Address:
307 Fukasaku, Minuma-ku, Saitama 337-8570, Japan

Brief Biographical History:
2011 Graduated Shibaura Institute of Technology
2011- Entered Graduate School of Engineering, Shibaura Institute of Technology

Membership in Academic Societies:
- The Japan Society of Mechanical Engineers (JSME)

Name:
Shozo Saegusa

Affiliation:
Professor, Hiroshima University

Address:
VBL office, 2-313 Kagamiyama, Higashi-Hiroshima 739-8527, Japan

Brief Biographical History:
1975- Joined Mechanical Engineering Research Laboratory, Hitachi, Ltd.
2005- Collaborative Research Center, Hiroshima University

Main Works:
- "Development of a guide-dog robot: human-robot interface considering walking conditions for a visually handicapped person," Microsystem Technologies, Vol.17, Issue 5, pp. 1169-1174, 2011.

Membership in Academic Societies:
- The Japan Society of Mechanical Engineers (JSME), Fellow
- American Society of Mechanical Engineers (ASME), Member
- Society of Instrument and Control Engineers (SICE)
- The Japan Society for Science Policy and Research Management

Name:
Kazuhisa Ito

Affiliation:
Professor, Department of Machinery and Control Systems, College of Systems Engineering and Science, Shibaura Institute of Technology

Address:
307 Fukasaku, Minuma-ku, Saitama 337-8570, Japan

Brief Biographical History:
2001- Assistant Professor, Sophia University
2007- Associate Professor, Tottori University
2009- Associate Professor, Shibaura Institute of Technology
2011- Full Professor, Shibaura Institute of Technology

Main Works:
- "Development of Articulated Manipulators with Pneumatic Cylinders," Int. J. of Automation Technology, Vol.5, No.4, pp. 478-484, 2011.

Membership in Academic Societies:
- The Japan Fluid Power System Society (JFPS)
- The Society of Instrument and Control Engineers (SICE)
- The Japan Society of Mechanical Engineers (JSME)
- The Institute of Electrical Engineers of Japan (IEEJ)

Name:
Louis Yuge

Affiliation:
Professor, Division of Bio-Environmental Adaptation Sciences, Graduate School of Biomedical & Health Sciences, Hiroshima University

Address:
1-2-3 Kasumi, Minami-ku, Hiroshima 734-8551, Japan

Brief Biographical History:
1999 M.Sc. from the Graduate School of Health Sciences, Hiroshima University
2000 Dr.Med.Sc./Ph.D. from the Graduate School of Biomedical Sciences at Hiroshima University

Main Works:
- "Simulated microgravity maintains the undifferentiated state and enhances the neural repair potential of bone marrow stromal cells," Stem Cells Dev, Vol.20, pp. 893-900, 2011.
- "Neuromagnetic beta oscillation changes during motor imagery and motor execution of skilled movements," Neuroreport, Vol.22, pp. 217-222, 2011.

Membership in Academic Societies:
- International Society for Stem Cell Research
- International Brain Mapping & Intraoperative Surgical Planning Society
- The Japanese Physical Therapy Association
- The Japanese Society for Regenerative Medicine